PLOS ONE

RESEARCH ARTICLE

Identification of a distal RXFP1 gene enhancer with differential activity in fibrotic lung fibroblasts involving AP-1

Ting-Yun Chen[1,2☯], Xiaoyun Li[1☯], Gillian C. Goobie[1,3,4], Ching-Hsia Hung[2], Tin-Kan Hung[5], Kyle Hamilton[1], Harinath Bahudhanapati[1], Jiangning Tan[1], Daniel J. Kass[1], Yingze Zhang[1,4,5]*

1 Division of Pulmonary, Allergy and Critical Care Medicine and The Dorothy P. and Richard P. Simmons Center for Interstitial Lung Disease, University of Pittsburgh, Pittsburgh, PA, United States of America, **2** Institute of Allied Health Sciences, National Cheng Kung University, Tainan, Taiwan, **3** Department of Medicine, Clinician Investigator Program, University of British Columbia, Vancouver, B.C., Canada, **4** Department of Human Genetics, Graduate School of Public Health, University of Pittsburgh, Pittsburgh, PA, United States of America, **5** Department of Bioengineering, Swanson School of Engineering, University of Pittsburgh, Pittsburgh, PA, United States of America

☯ These authors contributed equally to this work.
* zhanyx@upmc.edu

Citation: Chen T-Y, Li X, Goobie GC, Hung C-H, Hung T-K, Hamilton K, et al. (2021) Identification of a distal RXFP1 gene enhancer with differential activity in fibrotic lung fibroblasts involving AP-1. PLoS ONE 16(12): e0254466. https://doi.org/10.1371/journal.pone.0254466

Editor: Chun-Hsi Huang, Southern Illinois University, UNITED STATES

Received: June 22, 2021

Accepted: December 13, 2021

Published: December 31, 2021

Data Availability Statement: All relevant data are within the manuscript and its Supporting Information files.

Funding: Funded by National Institute of Arthritis and Musculoskeletal and Skin Diseases (NIAMS) R21AR076024-01 (YZ) and pilot grant from 5P50AR060780-08 (YZ); Ministry of Science and Technology in Taiwan (MOST) 108IPFA0900005 (TYC). The funders had no role in study design, data collection and analysis, decision to publish, or preparation of the manuscript.

Abstract

Relaxin/insulin-like family peptide receptor 1 (RXFP1) mediates relaxin's antifibrotic effects and has reduced expression in the lung and skin of patients with fibrotic interstitial lung disease (fILD) including idiopathic pulmonary fibrosis (IPF) and systemic sclerosis (SSc). This may explain the failure of relaxin-based anti-fibrotic treatments in SSc, but the regulatory mechanisms controlling *RXFP1* expression remain largely unknown. This study aimed to identify regulatory elements of *RXFP1* that may function differentially in fibrotic fibroblasts. We identified and evaluated a distal regulatory region of *RXFP1* in lung fibroblasts using a luciferase reporter system. Using serial deletions, an enhancer upregulating pGL3-promoter activity was localized to the distal region between -584 to -242bp from the distal transcription start site (TSS). This enhancer exhibited reduced activity in IPF and SSc lung fibroblasts. Bioinformatic analysis identified two clusters of activator protein 1 (AP-1) transcription factor binding sites within the enhancer. Site-directed mutagenesis of the binding sites confirmed that only one cluster reduced activity (-358 to -353 relative to distal TSS). Co-expression of FOS in lung fibroblasts further increased enhancer activity. *In vitro* complex formation with a labeled probe spanning the functional AP-1 site using nuclear proteins isolated from lung fibroblasts confirmed a specific DNA/protein complex formation. Application of antibodies against JUN and FOS resulted in the complex alteration, while antibodies to JUNB and FOSL1 did not. Analysis of AP-1 binding in 5 pairs of control and IPF lung fibroblasts detected positive binding more frequently in control fibroblasts. Expression of *JUN* and *FOS* was reduced and correlated positively with *RXFP1* expression in IPF lungs. In conclusion, we identified a distal enhancer of *RXFP1* with differential activity in fibrotic lung fibroblasts involving AP-1 transcription factors. Our study provides insight into *RXFP1* downregulation in fILD and may support efforts to reevaluate relaxin-based therapeutics alongside upregulation of *RXFP1* transcription.

Competing interests: The authors have declared that no competing interests exist.

Introduction

Pulmonary fibrosis is a hallmark of fibrotic interstitial lung diseases (fILD). Although the pathogenesis of fILD is not fully understood [1], fibroblast activation in the lungs of patients with fILD results in aberrant extracellular matrix (ECM) collagen accumulation [2]. Idiopathic pulmonary fibrosis (IPF) and systemic sclerosis (SSc) are two of the most common types of fILD. IPF is a chronic and progressive disease associated with high morbidity and mortality [1, 2]. In patients with SSc, fILD is the disease manifestation associated with the highest mortality [3]. Despite the increasing global burden of fILD [4, 5], our understanding of the mechanisms underlying the development and progression of fibrosis and our ability to target these pathogenic pathways is lacking.

Relaxin is a heterodimeric peptide hormone that regulates collagen metabolism and ECM turnover [6]. Relaxin was considered to be a potent anti-fibrotic agent [7–11], but clinical studies have failed to show beneficial anti-fibrotic effects in patients with SSc [12]. Relaxin mediates its cellular effects through its receptor, Relaxin/insulin-like family peptide receptor 1 (RXFP1) [13]. It plays an important homeostatic role in tissue remodeling, for example through collagen relaxation of pelvic ligaments during parturition [14]. In fibrotic diseases, the relaxin/RXFP1 axis is dysregulated [14]. *RXFP1*-null mice develop early onset peribronchiolar and perivascular fibrosis, with *relaxin* knock out mice developing early pulmonary and systemic organ fibrosis [15, 16]. *RXFP1* expression is downregulated in whole lung tissue and lung fibroblasts from patients with fILD, including IPF and SSc [17–20]. *In vitro* studies of fibroblasts isolated from IPF and SSc lungs demonstrates minimal responsiveness to relaxin treatment in reducing extracellular matrix accumulation, but restoration of *RXFP1* expression restores the anti-fibrotic effects in these cells [17]. However, transcriptional regulation of *RXFP1* in fibroblasts is poorly understood. Characterization of *RXFP1* regulation will provide insight to therapeutic targets for restoring relaxin's anti-fibrotic effects in patients with fILD [14].

Activator protein 1 (AP-1) belongs to the superfamily of basic leucine zipper DNA-binding transcription factors. It exists as a dimer mainly consisting of two subfamilies: Fos and Jun subunits [21]. AP-1 targets the TPA response element (TRE, also known as the AP-1 site) that regulates gene expression in response to physiologic and pathologic functions [22]. This includes the transcriptional upregulation of genes important for tissue remodeling [23]. AP-1 also plays a central role in enhancer repertoires selection in fibroblasts, which are critical for tissue differentiation during development [24]. There is limited research to date investigating the role of AP-1 superfamily transcription factor regulation of *RXFP1*.

In this study, we sought to characterize the regulatory regions of the *RXFP1* gene and to identify transcriptional elements important in its regulation. Through fine mapping of these regions, we identified a novel distal enhancer containing specific binding motifs for AP-1. We further demonstrated direct binding of AP-1 to the *RXFP1* regulatory elements using *in vitro* models. Our study provides insight to the transcriptional regulation of *RXFP1* in lung fibroblasts, which may have future implications for relaxin-based therapeutics.

Methods

Cell culture

The study was approved and was determined to be "non-human" study by the Institutional Review Board at the University of Pittsburgh (STUDY18100070). Donor lungs were obtained from the CORE (Center for Organ Recovery and Education). IPF and SSc explanted lungs were recovered from patients who underwent lung transplantation at the University of Pittsburgh Medical Center. Donor and explanted lungs were de-identified and no potentially

identifying genetic information were collected from these tissues. Lung fibroblast lines derived from these lungs were maintained in Dulbecco's modified Eagle's medium (DMEM) with 10% fetal calf serum and 50 μg/mL penicillin-streptomycin (Thermo Fisher Scientific Inc.) at 37˚C and 5% CO_2.

Plasmids and cloning

Polymerase chain reaction (PCR) products were gel purified using Qiagen QlAquick gel purification columns (Qiagen) according to the manufacturer's instructions. The PCR products were cloned using promoter-less pGL3-basic (pB) vector or pGL3-promoter (pP) vector containing a SV40 promoter (Promega Corporation) and Gibson Assembly (New England BioLabs). The relative location and size of *RXFP1* DNA in each luciferase reporter plasmid are listed in S1 Table. Expression plasmid for human FOS, pLX304-FOS-V5, a gift from William Hahn (Addgene plasmid #59140 (http://n2t.net/addgene:59140) [25] was used for the co-transfection experiments with RXFP1 luciferase reporters.

Dual luciferase assay

Fibroblasts were seeded at 5,000 cells/well in 24 well cell culture plates and cultured overnight prior to transfection with either the pGL3-*RXFP1* reporter plasmids alone (0.4μg/well) or co-transfection with a transcription factor expression plasmid (0.3μg pGL3-*RXFP1* reporter and 0.1μg expression plasmid per well). A Renilla luciferase vector (pGL4.74 [hRluc/TK]) was used as a control (0.001μg/well, Promega) for transfection efficiency. Plasmids were transfected into primary lung fibroblasts using Lipofectamine 2000 according to the manufacturers' instruction. At 40 hours post-transfection, the cells were washed with PBS, lysed in 1 × passive lysis buffer and analyzed using the Dual-Luciferase Reporter Assay System (Promega Corporation) and a SpectraMax L Microplate Reader (Molecular Devices, LLC.). Relative expression levels of pGL-*RXFP1* reporters were normalized against pB or pP vector luciferase activity. Four independent fibroblast lines from each group (control, IPF and SSc) were used in this study. Transfection studies were performed with a minimum of duplicates in each experiment.

Prediction of putative promoter and TATA element

DNA sequences upstream of both distal and proximal transcriptional start sites (TSS) were used to identify putative promoter and TATA elements. The Neural Network Promoter Prediction method (http://www.fruitfly.org/seq_tools/promoter.html) was used with a minimum promoter score of 0.85 [26]. This predictive tool was developed using both Drosophila and human consensus promoter sequences. The location of each identified element was determined based on the corresponding TSS.

Site-directed mutagenesis

Site-directed mutagenesis of the AP-1 binding sites in the distal enhancer reporter plasmids were performed using the Q5® Site-Directed Mutagenesis Kit (New England BioLabs). Primer pairs `5′-CCATAATGTGgggCTATACTAAATTTCATCTTC-3′` and `5′-CTAAATCCACTTAGAAAAAACAATC-3′`; `5′-AGCATGCATGgggCACAGATTGTTC-3′` and `5′-AAATGTAGCCAAACCCAG-3′` were used for binding site 1 and site 2, respectively.

Nuclear protein extraction

Nuclear proteins were prepared using fibroblasts at 80–90% confluency and the Nuclear Extract Kit (Active Motif), according to the manufacturer's protocol.

Electrophoretic Mobility Shift Assay (EMSA) and supershift analysis

A 37-base pair (bp) double-stranded oligonucleotide containing the AP-1-binding motif (underlined) of the *RXFP1* enhancer (5′-TACATTTAGCATGCATGACTCACAGATTGTTC TAGA-3′) was used as a probe for EMSA. The probe was biotin labeled at the 3' end using a Pierce™ Biotin 3' End DNA Labeling Kit (Thermo Fisher Scientific Inc.). EMSA were performed using the LightShift™ Chemiluminescent EMSA Kit (Thermo Fisher Scientific Inc.). Briefly, 2μl 10X binding buffer (100mM Tris, 500mM KCl, 10mM DTT; pH 7.5), 1μl poly (dI·dC) at 1μg/μl, 1μl 50% glycerol, 1μl 1% NP-40, 20fmol biotin-labeled probe and 7μg of nuclear proteins were mixed in a 20μl final volume and incubated at room temperature for 20 minutes. After incubation, 5μL of 5X loading buffer was added to each binding reaction and 20μL was immediately used for polyacrylamide gel electrophoresis (5% TBE precast polyacrylamide gel, Bio-Rad Laboratories, Inc.). The gel was transferred to a nylon membrane and DNA was crosslinked to the membrane with a hand-held 254nm UV lamp. After treated with blocking buffer, the membrane was incubated with streptavidin-horseradish peroxidase conjugate followed by an incubation with Luminol/Enhancer and peroxide solution prior to autoradiography with a CCD camera. For competition binding reaction, unlabeled wildtype, described above, or mutated AP-1 binding site probe at the underlined lowercase nucleotides (5′-TACATTTAGCATGCATGgggCACAGATTGTTCTAGA-3′) was added in 50-fold excess to the reaction mixture. Supershift assays were performed by incubating monoclonal antibody (Ab) to specific AP-1 transcription factors c-Jun (60a8, Cell Signaling), c-Fos (9F6), FOSL1 (Fra-1, D-3), and JUNB (C-11) from Santa Cruz Biotechnology with nuclear proteins for 10 minutes on ice and 10 minutes at room temperature prior to the binding reaction described above. Rabbit IgG (Cell Signaling) was used as a negative control. A total of 4 independent control and 4 IPF fibroblast lines were used for the binding analyses. Supershift analyses were conducted in nuclear protein isolated from 2 IPF and 2 control fibroblast lines.

Chromatin immunoprecipitation (ChIP) assay

ChIP assay was performed as described [27, 28]. Briefly, lung fibroblasts were grown on 100-mm tissue culture dishes to 90% confluence. Cells were cross-linked with 1% formaldehyde for 10 minutes and harvested for fragmentation using sonication. The chromatin fragments were immunoprecipitated with 3μg of the indicated antibodies for c-JUN (Cell signaling) and rabbit normal IgG (Cell signaling). The precipitated fragments were washed five times and analyzed by PCR using a primer pair (F: 5′- AAACACTGGACTGGGTTTG G-3′ and R: 5′- GGAAAGTAGGCCCCTTGAGA-3′) spanning the putative AP-1 binding site 2 on the *RXFP1* enhancer. ChIP assay was performed using rabbit IgG as a negative control. Densitometry analysis of the PCR amplification was performed using ImageJ [29]. Positive binding by JUN to the AP-1 site was estimated by JUN/IgG density using an arbitrary cutoff of 1.25. A total of 10 independent lung fibroblast lines (5 IPF and 5 control) were analyzed.

Western blot analysis

Lung fibroblasts were cultured to confluence and total proteins were prepared using radioimmunoprecipitation assay (RIPA). Proteins were separated by SDS-PAGE gel electrophoresis, transferred to polyvinylidene difluoride (PVDF) membrane (Bio-Rad), and blocked in 5% milk prior to primary antibody binding. Antibodies specific for JUN (Cell signaling technology, 9165) and FOS (Protein tech, 66590-1-IG) were used. Antibody for GAPDH (Abcam, ab181602) were used to determine sample loading. Membrane was developed using HRP-substrate (Millipore, Billerica, MA) and imaged using Amersham Imager 680 (GE Healthcare,

Marlborough, MA). The ImageJ software (National Institutes of Health) was used to perform densitometry analysis of the protein bands [29]. A total of 10 independent lung fibroblast lines (5 IPF and 5 control) were analyzed.

RXFP1 and AP-1 gene expression

Lung tissue-specific expressions of *RXFP1*, *JUN*, and *FOS* genes (where *JUN and FOS* are both AP-1 transcription factors) were obtained from the publicly available Lung Genomics Research Consortium (LGRC) gene expression dataset (GEO accession GSE47460; http://www.lung-genomics.org/) [30]. *FOS* gene expression was analyzed using microarray and was available for 108 controls and 160 IPF patients. *JUN* gene expression was only available from the RNA sequencing (RNAseq) dataset for 22 controls and 22 IPF patients. The expression levels on RNAseq were shown in Fragments Per Kilobase of transcript per Million mapped reads (fPKM) and were square root transformed for normality prior to analysis.

Statistical analysis

All data were expressed as the mean ± SD. Student's *t*-test was used for two-way comparisons. Gene expression levels of control and IPF groups were compared using the Mann-Whitney U test. Correlation of *FOS* and *JUN* gene expression levels with *RXFP1* expression levels was analyzed using linear regression modeling as described [31]. All analyses were performed in Prism GraphPad version 7 and a p value < 0.05 significance threshold was used.

Results

Identification of a functional promoter associated with distinct RXFP1 transcripts

RXFP1 is located on chromosome 4 (hg38, chr4:158,521,714–158,653,367) and historically was thought to be solely comprised of a 132kb (kilobase pair) genomic sequence (designated as the "Short" form of *RXFP1*). Subsequently the GENCODE project reported one extended *RXFP1* transcript with 204.6kb additional sequences (hg38, chr4:158,315,311–158,652,212) upstream of the previously reported transcript as shown in the University of California Santa Cruz (UCSC) genome browser (https://genome.ucsc.edu/). This is designated as the "Long" form of *RXFP1* (https://www.gencodegenes.org/). As shown in Fig 1A, there are multiple splicing variants associated with Short *RXFP1* [14], while only one transcript is associated with the Long form.

To determine whether a functional promoter is associated with each of the two forms of *RXFP1*, we analyzed the core promoter regions of each transcript using a pGL3 luciferase reporter system and primary lung fibroblasts isolated from donor lungs, as controls, and IPF lungs. A 233bp DNA element spanning -142 to +90 of the distal TSS (hg38, chr4:158,315,311) for the Long form (distal promoter), and a 194bp fragment covering -145 to +48 of the proximal TSS (hg38, chr4:158,521,714) for the Short form (proximal promoter) were tested (hereafter, all sequence locations are numbered relative to its corresponding TSS). As shown in Fig 1B, the distal promoter showed increased activity compared with pB vector, a promoter-less vector for testing promoter activity of targeted sequences, in both control and IPF lung fibroblasts ($p = 0.004$ and 0.002, respectively). In contrast, the reporter activities for the proximal promoter in both control and IPF fibroblasts were reduced compared with the pB vector although luciferase activities from both were very low.

We further analyzed the two promoter regions for chromatin characteristics associated with active transcriptional regulation including H3K4Me1, H3K27Ac, H3K4Me3 and DNAse

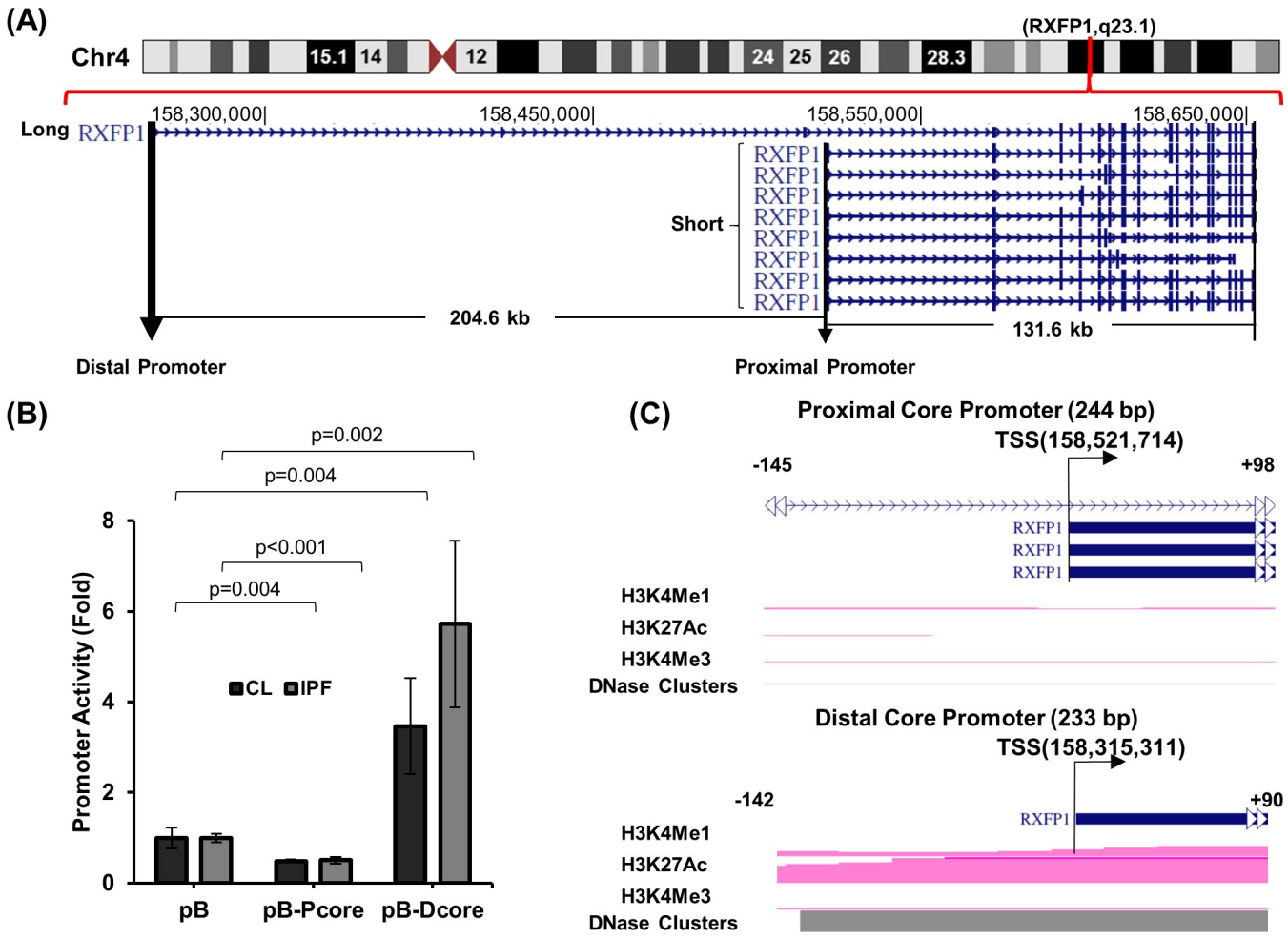

Fig 1. The genomic structure of *RXFP1* and core promoter activity. (A) Location of the Long and Short forms of *RXFP1* with identification of their mapped transcripts on chromosome 4 is shown. Genomic locations were determined based on the human genome build hg38 (https://genome.ucsc.edu/). The putative proximal and distal promoters are shown. (B) Proximal and distal core (P-Core and D-core, respectively) promoter activity analysis using a Luciferase promoter reporting system is shown. Transfections were performed in quadruplicates using Lipofectamine 2000 (Thermo-Fisher). Both control (CL) and idiopathic pulmonary fibrosis (IPF) lung fibroblasts were used. The promoter activity (fold) was calculated using pGL3basic (pB) as a control. Three control and 3 IPF independent lung fibroblast lines were tested and results from a representative experiment are shown as mean ± standard deviation. P-values for pairwise comparison using student T-test (two tailed) are shown. (C) Chromatin characteristics associated with active transcriptional regulation including H3K4Me1, H3K27Ac, H3K4Me3 and DNAse sensitivity clusters for the P-Core and D-Core region identified using the Encyclopedia of DNA Elements (ENCODE) histone ChIP data (https://genome.ucsc.edu/) are shown. The nucleotide location relative to each of the transcription start sites (TSS) are labelled. *RXFP1*, Relaxin/insulin-like family peptide receptor 1; UCSC, University of California, Santa Cruz.

https://doi.org/10.1371/journal.pone.0254466.g001

sensitivity clusters using the Encyclopedia of DNA Elements (ENCODE) histone ChIP data tracts in the UCSC genome browser (Fig 1C). Consistent with the reporter assay, only the distal promoter region was associated with positive transcriptional regulation signals, indicating that this was the only functional core promoter for the *RXFP1* gene in lung fibroblasts.

Differential distal promoter activities between control and fibrotic lung fibroblasts

Given the lack of promoter activity in the core proximal regulatory region, we extended our search for potential regulatory elements to both the proximal (PE) and distal (DE) regulatory regions. We analyzed the likelihood of a functional promoter by identifying a TATA box in a

3.1kb region (-2158bp to +971bp) and a 1.4kb region (-1202bp to +161bp) within the DE and PE regions, respectively. These regions possess potential regulatory functions based on the UCSC genome browser. Consistent with the lack of proximal promoter activity, there was no TATA box within 200bp upstream of the proximal TSS. However, a potential site was identified in the proximal region at -1095 to -1114. For the distal region, a TATA box was identified at -16 to +3 in addition to another site between -1946bp to -1927bp (Fig 2A).

These extended regions were further characterized in lung fibroblasts from control, IPF, and SSc patients for promoter activity using pB. Similar to the proximal core promoter, there was no increased activity for the PE in any fibroblast lines compared to the pB vector (Fig 2B). The 3.1kb DE retained its promoter activity and was always significantly increased compared to vector pB in all fibroblasts tested.

We performed serial deletions of the 1.4kb PE to rule out any repressor element interfering with promoter activity. Deleting 274 bp or 700 bp upstream sequences did not result in any significant promoter activity increase compared to the pB vector (Fig 2C), further supporting that only the distal regulatory region has promoter function.

Localization of an enhancer region upstream of the distal promoter with differential activities in control and fibrotic lung fibroblasts

Since the extended distal region retained promoter activities among control and fibrotic fibroblasts, we tested whether the extended distal region was associated with enhancer function using pGL3promoter, which contains a SV40 promoter and used for testing enhancer activity of targeted sequences. Using control fibroblasts, we consistently observed greater than 50-fold enhancer activity in the distal region while there was no activity for the proximal extended region compared to the pP vector (Fig 2D). The DE retained its enhancer activity and always significantly increased compared to vector pP in all fibroblasts tested and greater enhancer activities were observed in control than IPF and SSc fibroblasts. Deletion of 570bp (DE-D1), 637bp (DE-D2) in the 5' sequences of the 3.1kb extended distal region retained 73 ± 11% and 44 ± 2% enhancer activity ($p = 0.008$ and <0.001, respectively) (Fig 2E). Deletion of an additional 690bp (DE-D3) and 1360bp (DE-D4) completely abolished the enhancer activity ($p<0.001$ for both), suggesting that the enhancer is localized to a 690bp region between -951 to -261 (designated as the distal *RXFP1* enhancer). This was confirmed with the additional deletion of 1233bp 3' sequences (DE-D2toD3) of the D2 clone that fully restored the 3.1kb enhancer activity (106 ± 6%).

Fine mapping of the distal enhancer region

The distal enhancer partially overlaps with a region of dense transcription factor binding sites (TFBS, https://genome.ucsc.edu/) (Fig 3A). Therefore, we constructed a 608bp (−675 to −68) clone based on the TF binding cluster and designated it as pP-TFBS. Direct comparison of the distal *RXFP1* enhancer (pP-D2toD3) and the TFBS element showed similar enhancer activities in control and SSc lung fibroblasts (Fig 3B).

The enhancer activities were significantly reduced in SSc compared to control fibroblasts. We performed serial deletion using the pP-TFBS to further map the enhancer region (Fig 3C). A 91bp deletion (TFBS-D1) slightly increased the enhancer activity (108 ± 13%), while further deletion of 92bp (TFBS-D2) retained only 65 ± 18% of the activity. The enhancer activity was almost fully abolished when an additional 104bp (TFBS-D3) and 231bp (TFBS-D4) were deleted (6 ± 0.5%, $p<0.001$ for both). Deletion of the proximal 515bp (TFBS-D5) and 425bp (TFBS-D6) completely abolished enhancer activity (3 ± 0.8% and 4 ± 0.3%, $p<0.001$ for both), while proximal 321bp deletion (TFBS-D7) resulted in 46 ± 2%($p = 0.005$) enhancer activity.

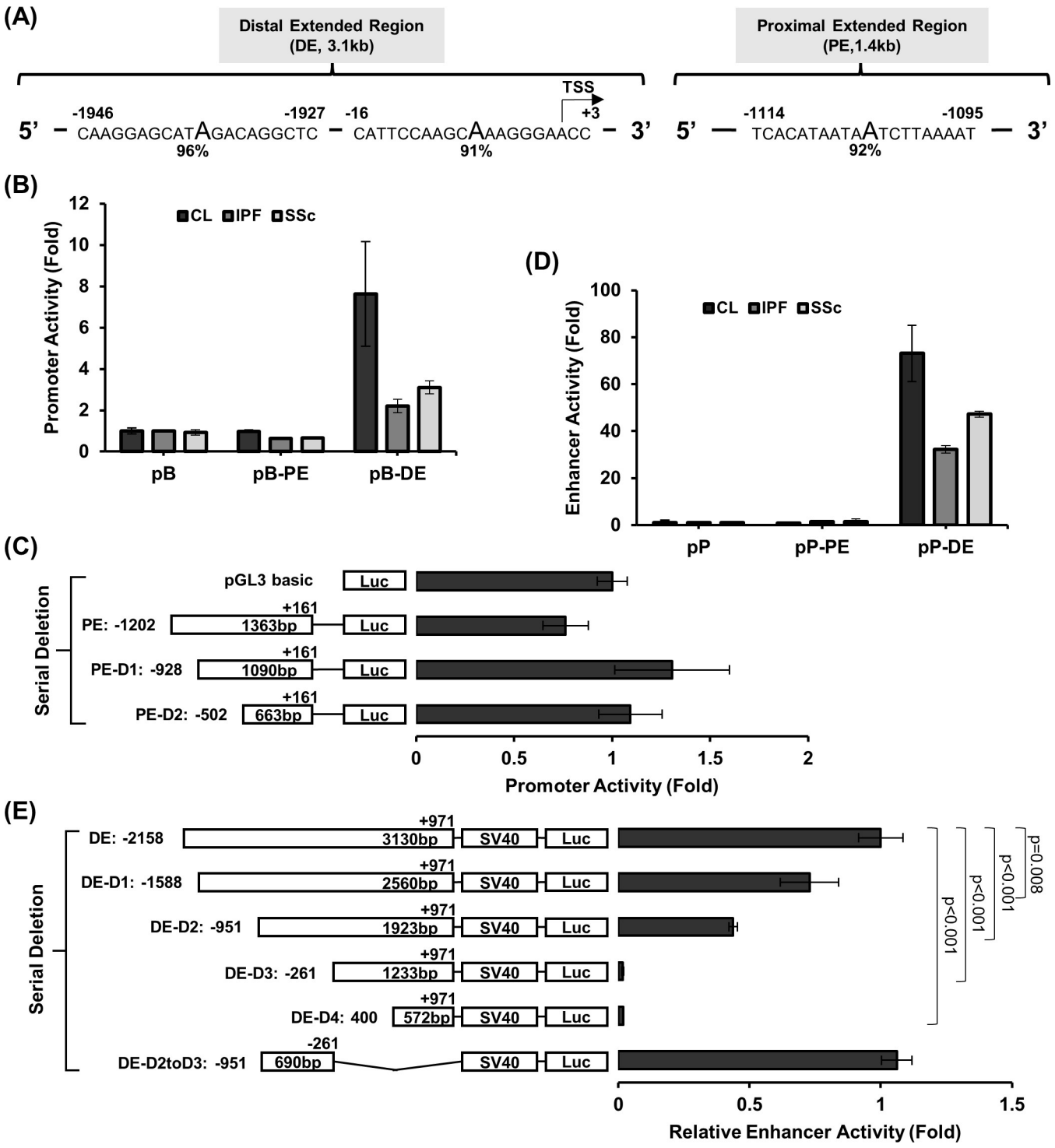

Fig 2. The promoter and enhancer activity in the extended proximal and distal regulatory regions. (A) Locations of TATA elements identified in the extended 3.1kb distal (DE) and 1.4kb proximal (PE) regulatory regions are shown using the Neural Network Promoter Prediction method (http://www.fruitfly.org/seq_tools/promoter.html). Relative nucleotide locations to the TSS are labelled. (B) Promoter activities of the extended proximal (pB-PE) and distal (pB-DE) regulatory regions with pGL3 promoter reporter system (transfections performed in duplicates) using control (CL), idiopathic pulmonary fibrosis (IPF) and systemic sclerosis (SSc) lung fibroblasts are shown. The transfection was performed in duplicates and fold changes relative to the pGL3basic (PB) vector are shown. Four control, 2 IPF, and 2 SSc independent lung fibroblast lines were tested and results from a representative experiment are shown as mean ± standard deviation. (C) Deletional analyses of the extended proximal regulatory region (PE-D1, proximal deletion 1; PE-D2, proximal deletion 2) using control fibroblasts. The transfection was performed in triplicates and tested in 1 control and 3 IPF independent lung fibroblast lines and results from a

representative experiment are shown as mean ± standard deviation. Fold changes are relative to the pGL3basic (pB) vector. (D) Enhancer activity of the extended proximal and distal regulatory regions with pGL3 enhancer reporter system (transfections performed in duplicates) using control, IPF and SSc lung fibroblasts are shown. Fold changes are relative to the pGL3promoter (pP) vector. (E) Serial deletion of the extended distal regulatory region is shown. The deletion plasmids are sequentially labeled as DE-D1 to DE-D4, and the plasmid with the sequence between DE-D2 and DE-D3 retained and a deletion of the retained sequence in DE-D3 is labeled as DE-D2toD3. The beginning and ending locations relative to the TSS and fragment size for each clone are labelled. Relative enhancer activities are calculated by determining the fold change using pP as a control for each reporter plasmid and subsequently using this to calculate the fold change between each plasmid to the original 3.1kb DE plasmid. The analyses in (D) and (E) were performed in 1 control, 1 IPF and 3 SSc independent fibroblast lines and results from a representative experiment are shown as mean ± standard deviation. For (E), p-values for pairwise comparisons of luciferase activity using student's T-test (two tailed) are shown.

https://doi.org/10.1371/journal.pone.0254466.g002

Lastly, deletion of proximal 193bp (TFBS-D8) resulted in stronger enhancer activity compared to the parental TFBS clone (149 ± 14%, p = 0.005). This mapped the distal enhancer to an area between -584 and -261bp from the distal TSS.

We further refined the enhancer region by serial deletion of the 515 bp TFBS-D1 clone (-584 to -68) from both 5' and 3' ends and tested the enhancer activity in control lung fibroblasts. Among all deletions, a 343bp element (-584 to -242, TFBS-C) resulted in a 5.8-fold (±0.6) increased activity compared to TFBS-D1 ($p<0.001$). Thus, the enhancer appears to reside in this 343bp region (Fig 3D).

Distal enhancer activity is partially mediated through AP-1

To identify transcription factors that may mediate the enhancer activity, we mined the UCSC genome browser and identified binding sites for multiple transcription factors (S1 Fig). Since AP-1 is known to be an important transcription factor in extracellular matrix metabolism [23], and also has multiple known binding sites, we searched for an AP-1 binding site within our 343bp enhancer region using PROMO [32]. Two clusters of AP-1 binding sites were identified at -525 to -520 (site 1) and -358 to -353 (site 2) (Fig 4A). To determine if one or both of the AP-1 sites were functional, we performed site-directed mutagenesis of each site (Fig 4B) individually and tested the enhancer activity. Similar to the reduced activity for TFBS in SSc, we observed significantly lower enhancer activity in IPF fibroblasts compared with controls for the pP-TFBS-C (IPF: 110.1 ± 15.6 and control: 217.4 ± 24.4 fold, $p<0.001$) (Fig 4C). Mutation of site 1 (pP-M1) retained the enhancer activity in control fibroblast (207.0 ± 8.1 fold) and resulted in a slightly reduced activity in IPF fibroblasts (94.2 ± 11.5 fold). Mutation of site 2 (pP-M2) partially abolished the activity in both control (649 ± 4.9 fold) and IPF fibroblasts (24.0 ± 2.4 fold, $p<0.001$ for both). Co-expression of a FOS expression plasmid with the 343 bp enhancer led to 5.4 ± 0.5 fold and 4.3 ± 0.3 fold ($p<0.001$ for both) increase in enhancer activities for control and IPF fibroblasts (Fig 4D). Similar transactivation by FOS was observed in control and IPF fibroblasts for the M1 mutation compare to the wildtype pP-TFBS-C, while only about two-fold increase in enhancer activity for the M2 mutation was observed in both fibroblasts (Fig 4D).

Direct binding of AP-1 to the distal enhancer

We further tested whether AP-1 factors directly bind to the enhancer using a labeled probe spanning the functional site 2 of AP-1 and nuclear proteins isolated from control and IPF lung fibroblasts. Compared to probe alone, addition of nuclear proteins resulted in a complex formation (complex A) which was competed out with 50-fold unlabeled wildtype probe, but not unlabeled AP-1 site mutated probe in the binding reaction (Fig 5A, lane 2–4). Supershift experiments with an antibody specific for JUN resulted in a higher molecular weight complex (Fig 5A and 5B, complex B). Antibody specific for FOS reduced the intensity of complex A, indicating the binding of antibody to FOS resulted in an interference to its binding to the AP-

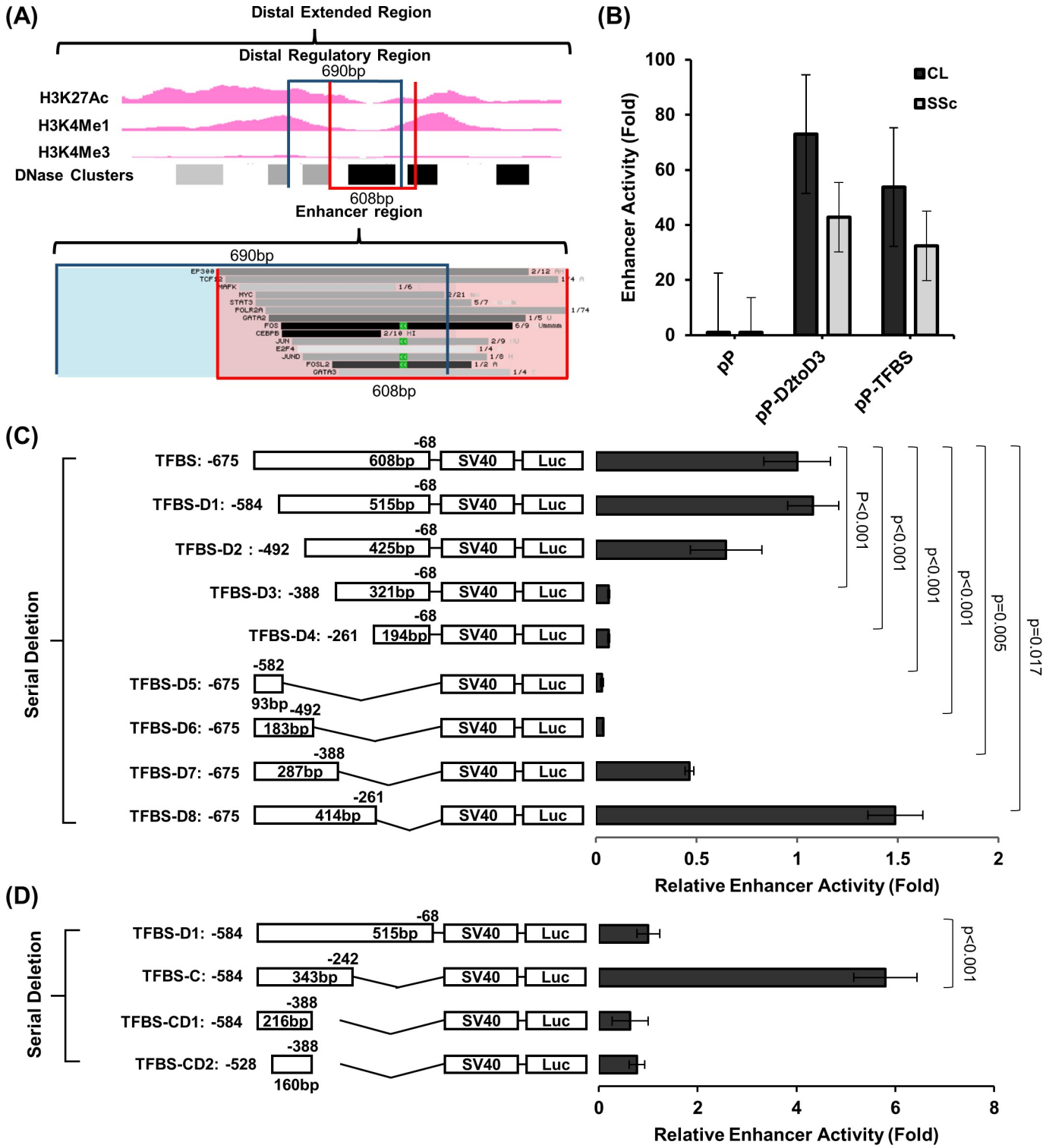

Fig 3. Fine mapping of the distal enhancer. (A) Chromatin characteristics including H3K4Me1, H3K27Ac, H3K4Me3 and DNAse sensitivity clusters for the region flanking the 690bp distal enhancer and the transcription factor binding sites (TFBSs) using UCSC genome browser are shown. (B) Enhancer activity of the 690bp (pP-D2toD3) and 608bp (pP-TFBS) distal enhancer (transfections performed in triplicates) using control and SSc lung fibroblasts with the pGL3promoter (pP) as a control are shown. The promoter activities of pP-D2toD3 and pP-TFBS were tested in 3 control and 3 SSc independent lung fibroblast lines and results from a representative experiment are shown as mean ± standard deviation. (C) and (D) Serial deletion of the 608bp (pP-TFBS) and 515bp (TFBS-D1) distal enhancer are shown. In (C) the deletion plasmids are sequentially labeled as TFBS-D1 to D8 and in (D), they are labelled as TFBS-C and TFBS-CD1 to CD2. Transfections were performed in triplicates. Relative enhancer activities are calculated by obtaining the fold change using pP as a control for each deletion

plasmid and subsequently using this to calculate the fold change using pP-TFBS (C) or TFBS-D1 (D) as respective controls. A minimum of 3 independent experiments were performed for (C) and (D) using 1 control and 1 IPF independent lung fibroblasts lines and results from a representative experiment using control are shown as mean ± standard deviation. For (C) and (D), p-values for pairwise comparisons of luciferase activity using student's T-test (two tailed) are shown.

https://doi.org/10.1371/journal.pone.0254466.g003

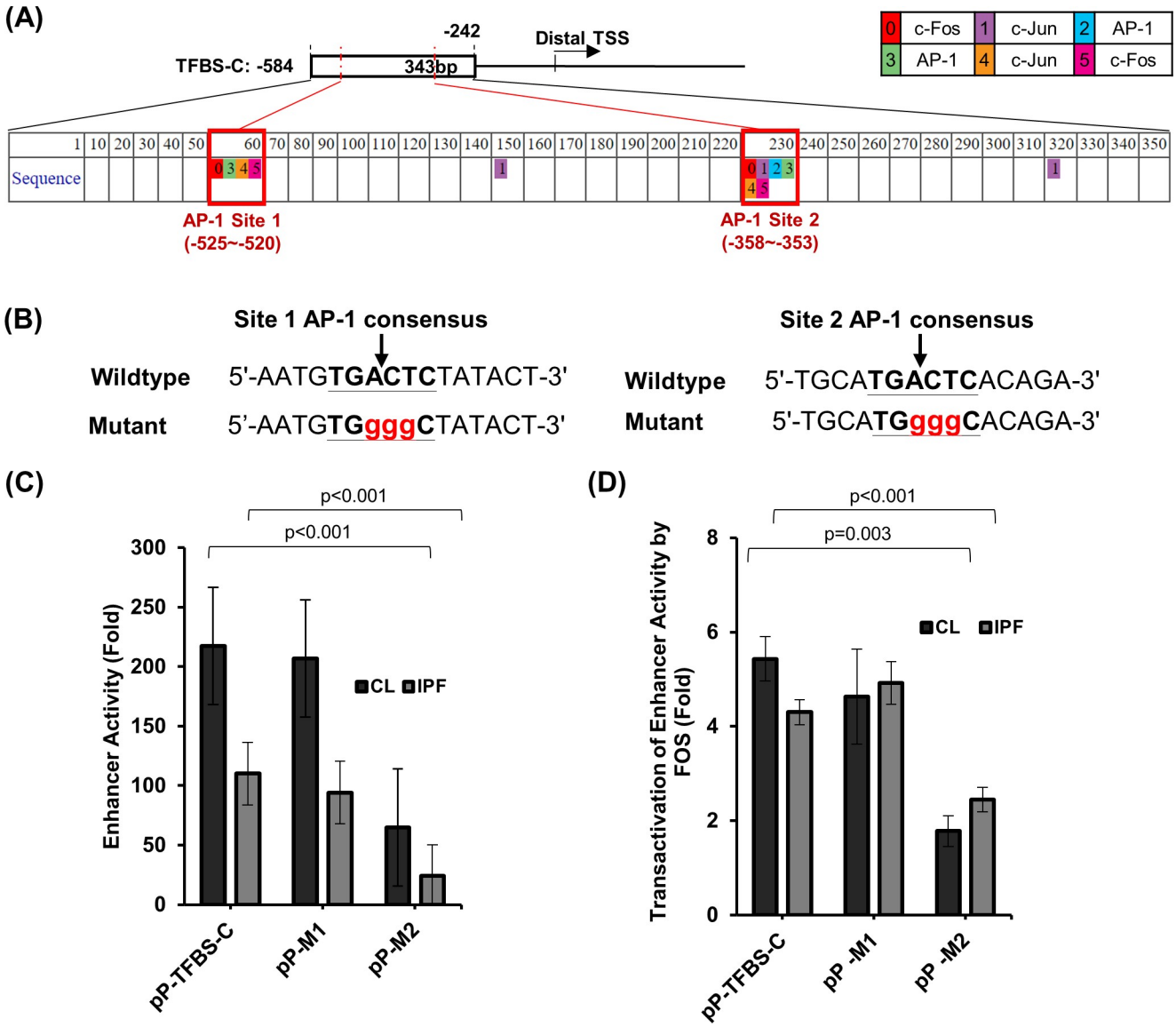

Fig 4. Functional AP-1 binding site associated with the distal enhancer. (A) Locations of AP-1 binding site clusters in the distal enhancer identified using the PROMO prediction online tool are shown. (B) Mutation of AP-1 consensus sequences for both site 1 and site 2. AP-1 sites are bolded and underlined. Mutated nucleotides are in red lower cases. (C) Enhancer activities of the pGL2promoter reporter plasmids with wildtype AP-1 or AP-1 site specific mutations in the distal *RXFP1* enhancer in control (CL) and idiopathic pulmonary fibrosis (IPF) lung fibroblasts. Vector pGL2promoter (pP) was used as a control. (D) Increases of enhancer activities of the wildtype and mutant AP-1 binding site reporters by over-expressing FOS in control and IPF lung fibroblasts are shown. A FOS expression plasmid driven by CMV promoter was co-transfected into the fibroblasts with each reporter. Co-transfection with pcDNA3 was used as a control to calculate the fold increase in enhancer activity by FOS. Three control and 3 IPF independent lung fibroblast lines were analyzed in quadruplicates in each experiment. Representative results from one control and one IPF are shown as mean ± standard deviation. For (C) and (D), p-values for pairwise comparisons of luciferase activity using student's T-test (two tailed) are shown.

https://doi.org/10.1371/journal.pone.0254466.g004

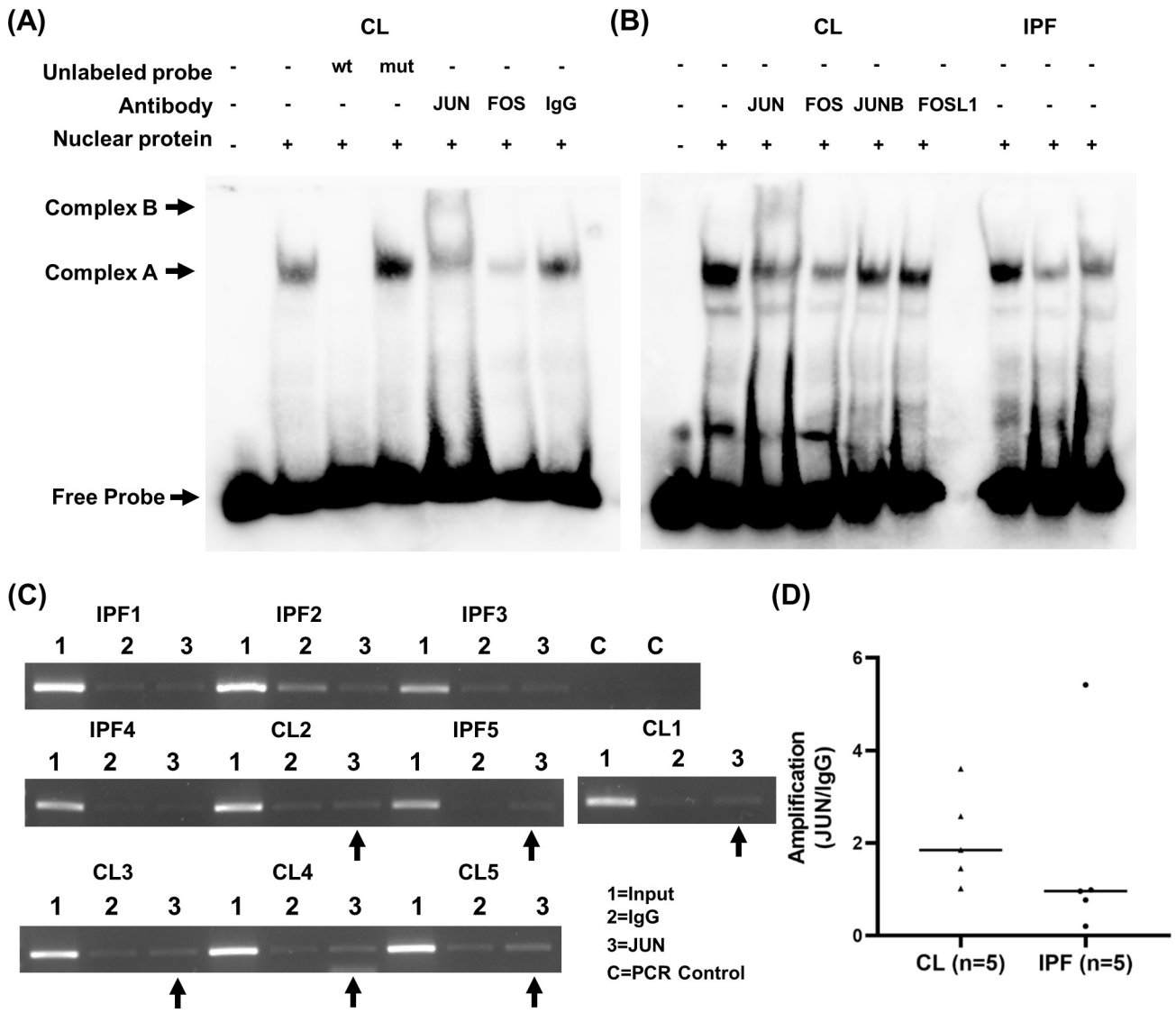

Fig 5. Direct binding of AP-1 to the RXFP1 distal enhancer. (A) Binding of JUN and FOS to the AP-1 site 2 analyzed using Electrophoretic Mobility Shift Assays (EMSA) and supershift analysis. Nuclear proteins isolated from control (CL) and IPF lung fibroblasts were used for the binding assay with a biotin-labeled 37-base pair double-stranded oligonucleotide containing the AP-1-binding motif site 2 of the *RXFP1* enhancer. The unlabeled wildtype (wt) or mutated (mut) AP-1 site probe at 50-fold of labeled wt *RXFP1* probe were used as unlabeled competitors for the specific binding competition assays. Supershift analyses with antibodies specific for JUN, FOS, JUNB and FOSL1 or control IgG are shown. The AP-1 specific complex is labeled as "complex A". The supershifted complex with antibody specific for JUN is labeled as "complex B". Unbound free labeled probe band is marked as "free probe". A total of 4 control and 4 IPF independent lung fibroblast lines were used for the binding analyses and results from 3 IPF and 1 control fibroblast lines are shown. Supershift analyses with antibodies specific for AP-1 factors were conducted in nuclear protein isolated from 2 IPF and 2 control fibroblast lines and results from one control fibroblast line are shown (B). (C) Chromatin Immunoprecipitation (ChIP) analysis of 5 independent control and 5 IPF lung fibroblast lines for JUN binding to the *RXFP1* distal enhancer. The distal enhancer region from -394 to -245 of distal TSS was amplified using DNA samples from pulldown samples by JUN antibody. Input and IgG pulldown products were used as controls. (D) Densitometry analyses of the PCR amplification from (C) using ImageJ are shown. Positive binding by JUN to the distal enhancer was estimated by JUN/IgG density using an arbitrary cutoff of 1.25 (25% increase in binding for JUN). Student's T-test (two tailed) was used for the pairwise comparison between IgG and JUN, and significance was not met.

https://doi.org/10.1371/journal.pone.0254466.g005

1 site or the formation of a larger complex which could not be separated by the polyacrylamide gel. The control rabbit IgG did not change the complex A formation. Analysis with additional AP-1 TF including JUNB and FOSL1 showed no supershifted complex and very little changes in the complex A intensity (Fig 5B). Nuclear proteins isolated from IPF fibroblasts resulted in

similar intensity of complex A formations as control fibroblasts (Fig 5B and S2B Fig). These suggest that JUN and FOS directly bind to the AP-1 site located at the -358 to -353 position in the distal enhancer.

ChIP analysis was performed using an antibody specific for JUN and 10 independent lung fibroblast lines (5 control and 5 IPF). To estimate the positive binding, we used an arbitrary cutoff of a 25% increase in PCR amplification for the pulldown ratio (JUN/IgG) >1.25 based on the densitometry analysis of the PCR amplification products with primers spanning the AP-1 binding site 2. For control fibroblast lines, 4/5 of them had pulldown signal while only 1/5 IPF lines was positive (Fig 5C) although direct two-group comparison did not meet statistical significance (1.67 ± 2.11 vs 2.10 ±1.02) (Fig 5D). These findings suggest that in comparison to control fibroblasts, there may be lower JUN binding to the functional AP-1 site of the *RXFP1* distal regulatory region in IPF fibroblasts. However, quantitative analysis of the *RXFP1* gene expression in each fibroblast did not show any correlation with observed binding level of JUN to the AP-1 site from the ChIP assay (S3 Fig).

Reduced expression of JUN and FOS in IPF lungs and direct correlations to RXFP1 gene expression

Microarray whole lung tissue gene expression was performed for 108 controls and 160 IPF in the LGRC dataset [30] for *FOS* and *RXFP1*. The demographic and clinical characteristics are shown in S2 Table. Patients with IPF had lower expressions of *FOS* compared to controls (15.2 ± 1.7 and 13.5 ± 1.6 normalized hybridization signal for controls and IPF, $p<0.001$) (Fig 6A). The expression levels of *FOS* were positively correlated with *RXFP1* expression in patients with IPF ($R^2 = 0.060$, $p = 0.002$) (Fig 6B). Since *JUN* expression was not included in the microarray dataset, we used the available bulk RNA sequencing (RNAseq) data from 22 controls and 22 patients with IPF. The expression levels of *JUN* showed reduced levels in IPF compared to controls (1377 ± 39.5 and 1053 ± 535 fPKM for controls and IPF, $p = 0.001$) (Fig 6C). The expression levels of *JUN* were also correlated to the levels of *RXFP1* analyzed using RNAseq ($R^2 = 0.365$, $p<0.001$) (Fig 6D) in IPF. As a control, the reduced expression of *FOS* in IPF and positive correlation with *RXFP1* expression levels were confirmed in the RNAseq dataset (S4A Fig).

To determine whether AP-1 expression is reduced in IPF fibroblasts, we analyzed the protein expressions of JUN and FOS in independent lung fibroblast lines (5 control and 5 IPF). The levels of FOS protein were reduced in IPF fibroblasts than controls (Fig 4E and 4F). Lower levels of JUN protein were also detected in IPF compared to controls without statistical significance.

Discussion

We have identified a strong enhancer within the distal regulatory region of *RXFP1*, which had reduced activities upon introduction into fibrotic lung fibroblasts compared to controls. The enhancer activity was partially mediated by AP-1, with lower expression of *JUN* and *FOS* in lungs from patients with IPF compared to controls and lower binding of JUN to the enhancer region in IPF fibroblasts. Furthermore, expression levels of *JUN* and *FOS* were positively correlated with *RXFP1* expression in lung tissue from patients with IPF. This is the first study to systemically analyze the regulatory elements of *RXFP1*, thus providing molecular insights into transcriptional regulation of this important protein in lung fibroblasts.

A number of studies support relaxin as a potent anti-fibrotic agent [7–11, 33, 34]. Relaxin enhances the degradation of ECM in tissues by upregulating members of the matrix metalloproteinase (MMP) family [35]. The failed clinical studies for relaxin-based treatments in SSc

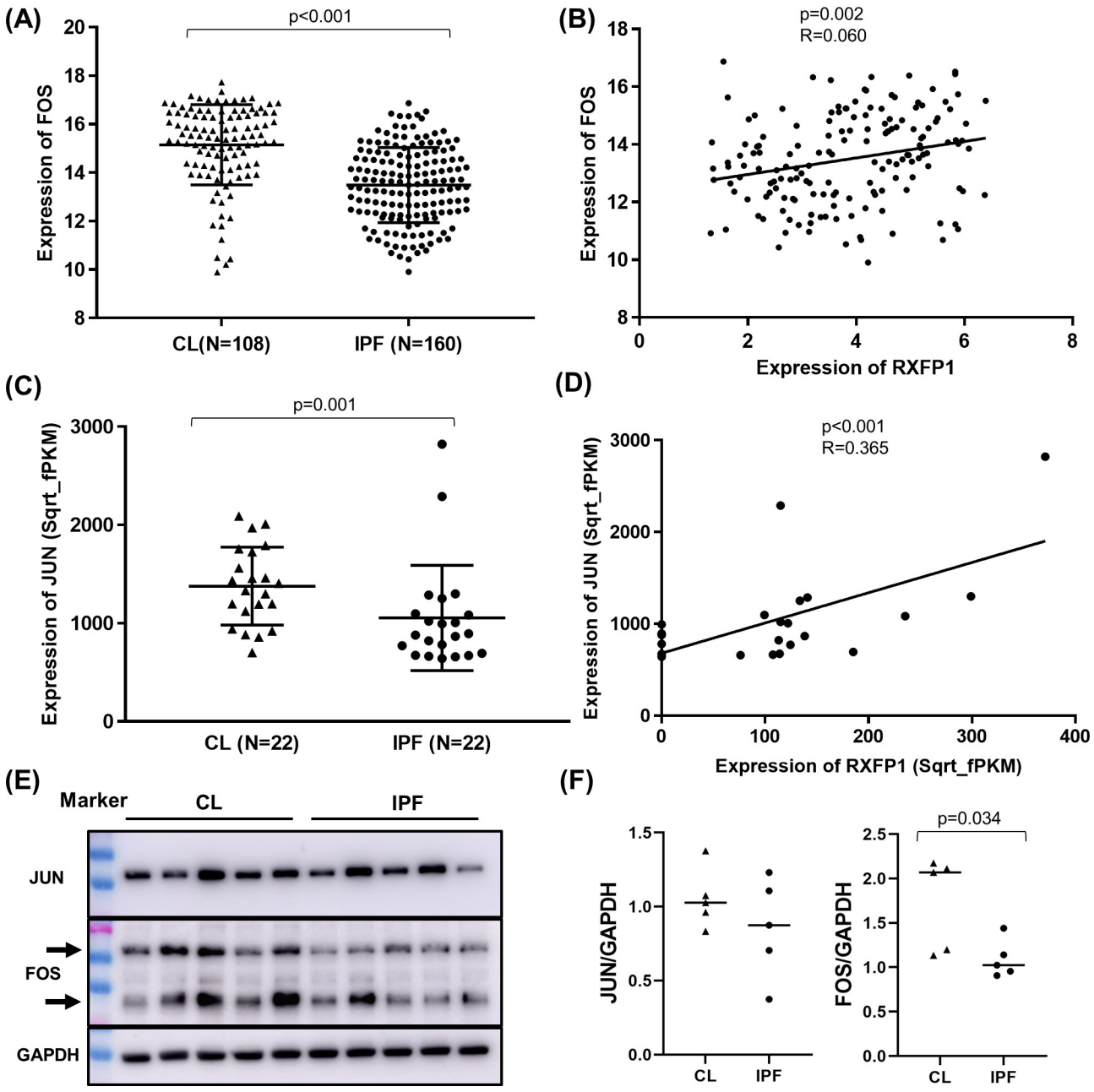

Fig 6. Lower expression of *JUN* and *FOS* and positive correlation to RXFP1 in control and IPF lungs and lung fibroblasts. Lung tissue expression levels of *FOS* analyzed using microarray (A) and *JUN* analyzed using bulk RNA sequencing (C) from the publicly available Lung Genomics Research Consortium (LGRC) gene expression dataset (GEO accession GSE47460; http://www.lung-genomics.org/) were compared between control (108 subjects for *FOS* and 22 subjects for *JUN*) and idiopathic pulmonary fibrosis (IPF) (160 subjects for *FOS* and 22 subjects for *JUN*). The mean and standard deviation for each group and Mann-Whitney U test p-values are shown. Correlation of *FOS* (B) and *JUN* (D) gene expression levels with *RXFP1* was analyzed in IPF lungs (160 subjects for *FOS* and 22 subjects for *JUN*) using linear regression and the R^2 and p-value are shown. (E) Protein levels of JUN and FOS in independent IPF and control lung fibroblast lines analyzed by western blot with antibodies specific for JUN (rabbit mAb, Cell signaling technology #9165) and FOS (mouse mAb, Protein tech # 66590-1-IG). GAPDH (rabbit mAb Abcam Abcam ab181602) was used as a sample loading control. Total proteins isolated from confluent fibroblasts using radioimmunoprecipitation assay (RIPA) were separated by SDS-PAGE gel electrophoresis. (F) Densitometry of the results on (E) using the ImageJ software (National Institutes of Health) [29]. For FOS, total density of both bands was used for each sample. A total of 10 independent lung fibroblast lines (5 IPF and 5 control) were analyzed.

https://doi.org/10.1371/journal.pone.0254466.g006

patients [12] may be related to reduced expression of *RXFP1* in fibroblasts of these patients, which would abrogate their responsiveness to relaxin [14, 17–19]. Patients with IPF and SSc with higher *RXFP1* expression in their lungs have better pulmonary function, supporting the pathophysiologic relevance of this locus in fILD [17]. *In vitro* silencing of *RXFP1* results in insensitivity to exogenous relaxin, an effect which is reversed by enhancement of *RXFP1* expression in both control and IPF lung fibroblasts [17]. In this context, upregulation of *RXFP1* may serve as a therapeutic option that would help to restore the responsiveness to relaxin-based therapies in fibrotic tissues [36]. Our study suggests that transcriptional modulation of *RXFP1* in fibroblasts from patients with fILD may be one of the strategies to restore *RXFP1* expression and the responsiveness to relaxin-based antifibrotic therapies in patients with IPF and SSc.

AP-1 is ubiquitously expressed in different cells and tissues and plays important roles in multiple cellular processes including proliferation, differentiation, senescence, and cell death [21, 37]. The AP-1 superfamily consists of four subfamilies, including FOS, JUN, ATF, and MAF, which exert their functions as homo- or hetero-dimers formed through their basic leucine-zipper (bZIP) motifs. The dimers formed with different AP-1 proteins are often associated with differential transcriptional regulation of target genes [38]. In general, the dimer of FOS and JUN is associated with positive gene regulation, while other family members such as JUNB act as negative transcriptional regulators [38]. Context dependent regulation by AP-1 transcription factors is also reported [37, 39]. AP-1 transcription factors can also preferentially bind to distal enhancers instead of promoters in regulating target genes [40], supporting the findings from this study. We identified FOS and JUN as positive regulators for the *RXFP1* gene distal enhancer in lung fibroblasts. The reduced *JUN* and *FOS* gene expression in IPF lungs and FOS protein expression in IPF lung fibroblasts suggest lower AP-1 expression may be one of the mechanisms associated with the decreased RXFP1 expression in fibrotic lungs. By upregulating these transcription factors in IPF fibroblasts we may be able to restore *RXFP1* expression and thus responsiveness to relaxin-based therapeutics in fibrotic fibroblasts. Interestingly, we did not observe a direct correlation of JUN binding by ChIP and *RXFP1* expression by quantitative PCR analysis in lung fibroblasts, suggesting other mechanisms are associated with RXFP1 gene regulation. This could be also due to the fact that ChIP represents a semi-quantitative measurement of DNA binding. Similarly, the binding of nuclear proteins to the AP-1 site was not different in IPF compared to control in our EMSA analysis although EMSA is also limited by being a semi-quantitative method.

Conversely, FOSL2, a member of the AP-1 FOS subfamily has been shown to exert profibrotic effects. Transgenic *Fosl2* mice develop spontaneous lung fibrosis with *Fosl2*-expressing macrophages promoting lung fibrosis [41, 42]. Interestingly, in the LGRC expression dataset, expression levels of *FOSL2* and *RXFP1* were negatively correlated (S4B Fig). Therefore, the differential effects on lung fibrosis between JUN and FOS from this study in fibroblasts and the *FOSL2* expression in mice macrophages illustrates the complexity of AP-1 family functions in lung fibrosis. Additionally, we found that miR-144-3p downregulates *RXFP1* expression through its 3'-untranslated region and that JUN was required for constitutive miR-144-3p expression in lung fibroblasts, suggesting that distinct functions may be associated with the same AP-1 factor depending on their partners for dimerization. Although it is out of the scope of this study, systematic analysis of different AP-1 members in regulating, positively or negatively, *RXFP1* expression is important for understanding the transcriptional regulation of this gene. The lack of regulatory functions in the proximal region of the *RXFP1* gene is surprising. We hypothesize that a potential mechanism may be through long-distance regulation of the proximal region by the distal enhancer, for example through chromatin conformation changes [43]. As reviewed by Bejjani and colleagues, genome-wide analysis has shown that AP-1

commonly binds the distal enhancers and regulates distant genes [40]. Although it is out of the scope of current study, analysis of the chromatin architecture in the *RXFP1* locus will be essential to determining whether AP-1 mediates distant control of the weak proximal regulatory region of *RXFP1* through this mechanism. In addition, reduced AP-1 binding to the *RXFP1* enhancer in IPF fibroblasts maybe due to the masking of the AP-1 binding site by differential DNA methylation in this locus in IPF fibroblasts. Therefore, characterization of epigenetic changes in fibrotic fibroblasts is warranted.

Our study does have some limitations. First, the analysis of *RXFP1* regulatory elements was mainly performed using primary fibroblasts from control, IPF and SSc lungs. We showed reduced direct binding of JUN to the *RXFP1* enhancer in lung fibroblasts using ChIP assay and positive correlation of *JUN* and *FOS* gene expression with *RXFP1* in IPF whole lung tissues, However, the gene expression levels in whole lung may mask the cell-type specific expression differences of these genes. However, the reduced FOS protein levels in IPF lung fibroblasts compared to controls supports that fibroblasts are an important cells type in mediating the lung specific functions of RXFP1. Second, we analyzed the *in vivo* binding of AP-1 to the *RXFP1* enhancer using limited number of fibroblast lines (5 control vs 5 IPF). Due to the heterogeneity of primary fibroblasts isolated from lungs [44], the interpretation of differences between groups such as the ChIP and EMSA assays in this study should be cautioned. Future analysis in additional fibrotic and control fibroblast lines may be helpful. Third, the AP-1 family consists of a large number of different transcription factors with both distinct and related functions [21, 37]. We only focused our analysis on JUN and FOS. Comprehensive analysis of other AP-1 family members in fibroblast *RXFP1* regulation is important.

In conclusion, we identified a distal enhancer of *RXFP1* with differential activity in fibrotic lung fibroblasts involving AP-1 transcription factors. Our study provides insight into the reduced expression of *RXFP1* in patients with IPF and may support efforts to restore the effectiveness of relaxin-based therapeutics in fILD through the upregulation of *RXFP1* transcription.

Supporting information

S1 Table. Genomic location and size of cloned RXFP1 fragments.
(DOCX)

S2 Table. Demographic and clinical characteristics of subjects from the LGRC study.
(DOCX)

S1 Fig. Transcription factor binding sites within distal enhancer region of the RXFP1. (A) chromatin characteristics associated with active transcriptional regulation including H3K4Me1, H3K27Ac, H3K4Me3 and DNAse sensitivity clusters using the Encyclopedia of DNA Elements (ENCODE) histone ChIP data tracts in the UCSC genome browser (https://genome.ucsc.edu/). (B) Transcription factors identified using the UCSC Genome Browser for the 608bp enhancer region. The narrowed 343bp enhancer was boxed in red. Nucleotide locations of the two AP-1 sites are labeled. The colored boxes with specific numbers correspond to specific transcription factors and detailed in (C).
(PDF)

S2 Fig. Original picture for EMSA in Fig 5A and 5B and additional EMSA using nuclear protein from control and IPF fibroblasts. (A) Original photos for the EMSA analysis showing in Fig 5A (left top) and 5B (right). The (A) left bottom was not used in the main text but was for an experiment performed at the same time as that for Fig 5A. Therefore, we included it for data integrity. The arrow indicates an artifact as it is located in between the two lanes. (B)

Independent EMSA analysis using nuclear proteins from control and IPF and not a part of the main figures. Nuclear proteins isolated from control (CL) and IPF lung fibroblasts were used for the binding assay with a biotin-labeled 37-base pair double-stranded oligonucleotide containing the AP-1-binding motif site 2 of the *RXFP1* enhancer. The unlabeled wildtype (wt) or mutated (mut) AP-1 site probe at 50-fold of labeled wt *RXFP1* probe were used as unlabeled competitor for the specific binding competition assays. Supershift analyses with antibodies specific for JUN, FOS, JUNB and FOSL1 or control IgG are shown. The AP-1 specific complex is labeled as "complex A". The supershifted complex with antibody specific for JUN is labeled as "complex B". Unbound free labeled probe band is marked as "free probe".
(PDF)

S3 Fig. Correlation of JUN binding in ChIP assay to *RXFP1* gene expression by qPCR. *RXFP1* gene expression was analyzed using a quantitative PCR (qPCR) with a Taqman probe (Hs01073141_m1) and standard protocol. The qPCR was analyzed using a QuantStudio 5 System (Applied Biosystem Inc.). Correlation of JUN binding analyzed by the ChIP analysis on Fig 5C and 5D was performed using the qPCR results in Graphpad 7 and no correlation was observed.
(PDF)

S4 Fig. FOS expression in IPF and control lungs and FOS and FOSL2 correlation to RXFP1 gene expression in LGRC. (A) Lung tissue expression levels of *FOS* in control and IPF (n = 22 for each) analyzed using bulk RNA sequencing from the publicly available Lung Genomics Research Consortium (LGRC) gene expression dataset (GEO accession GSE47460; http://www.lung-genomics.org/). Correlation of *FOS* (right) gene expression levels with *RXFP1* was analyzed in IPF lungs (22 subjects) using linear regression and the R^2 and p-value are shown. (B) Correlation of *FOSL2* gene expression levels with *RXFP1* was analyzed with microarray in IPF lungs (160 subjects) using linear regression and the R^2 and p-value are shown.
(PDF)

S5 Fig. Original DNA agarose gel images for the ChIP analysis Fig 5C. Agarose gel images from the gel electrophoresis for the Chromatin Immunoprecipitation (ChIP) analysis shown in Fig 5C. 1 = input, 2 = IgG, 3 = JUN antibody, C = PCR Control, CL = control fibroblast. Molecular weight markers are included for each gel.
(PDF)

S6 Fig. Original Western blot images Fig 6E. The bands specific for FOS, JUN and GAPDH are shown.
(PDF)

Author Contributions

Conceptualization: Ting-Yun Chen, Yingze Zhang.

Data curation: Ting-Yun Chen, Xiaoyun Li, Kyle Hamilton.

Formal analysis: Ting-Yun Chen, Xiaoyun Li, Gillian C. Goobie, Tin-Kan Hung, Yingze Zhang.

Funding acquisition: Yingze Zhang.

Investigation: Daniel J. Kass, Yingze Zhang.

Methodology: Xiaoyun Li, Harinath Bahudhanapati, Jiangning Tan.

Project administration: Yingze Zhang.

Supervision: Ching-Hsia Hung, Yingze Zhang.

Writing – original draft: Ting-Yun Chen, Xiaoyun Li, Yingze Zhang.

Writing – review & editing: Ting-Yun Chen, Gillian C. Goobie, Ching-Hsia Hung, Tin-Kan Hung, Kyle Hamilton, Harinath Bahudhanapati, Jiangning Tan, Daniel J. Kass, Yingze Zhang.

References

1. Mortimer KM, Bartels DB, Hartmann N, Capapey J, Yang J, Gately R, et al. Characterizing Health Outcomes in Idiopathic Pulmonary Fibrosis using US Health Claims Data. Respiration. 2020:1–11. Epub 2020/01/27. https://doi.org/10.1159/000504630 PMID: 31982886.
2. King TE, Pardo A, Selman M. Idiopathic pulmonary fibrosis. The Lancet. 2011; 378(9807):1949–61.
3. Tyndall AJ, Bannert B, Vonk M, Airo P, Cozzi F, Carreira PE, et al. Causes and risk factors for death in systemic sclerosis: a study from the EULAR Scleroderma Trials and Research (EUSTAR) database. Ann Rheum Dis. 2010; 69(10):1809–15. Epub 2010/06/17. https://doi.org/10.1136/ard.2009.114264 PMID: 20551155.
4. Disease GBD, Injury I, Prevalence C. Global, regional, and national incidence, prevalence, and years lived with disability for 354 diseases and injuries for 195 countries and territories, 1990–2017: a systematic analysis for the Global Burden of Disease Study 2017. Lancet. 2018; 392(10159):1789–858. Epub 2018/11/30. https://doi.org/10.1016/S0140-6736(18)32279-7 PMID: 30496104; PubMed Central PMCID: PMC6227754.
5. Collaborators GBDCoD. Global, regional, and national age-sex-specific mortality for 282 causes of death in 195 countries and territories, 1980–2017: a systematic analysis for the Global Burden of Disease Study 2017. Lancet. 2018; 392(10159):1736–88. Epub 2018/11/30. https://doi.org/10.1016/S0140-6736(18)32203-7 PMID: 30496103; PubMed Central PMCID: PMC6227606.
6. Wilkinson TN, Speed TP, Tregear GW, Bathgate RA. Evolution of the relaxin-like peptide family. BMC Evol Biol. 52005. p. 14.
7. Samuel CS, Royce SG, Hewitson TD, Denton KM, Cooney TE, Bennett RG. Anti-fibrotic actions of relaxin. Br J Pharmacol. 2017; 174(10):962–76. https://doi.org/10.1111/bph.13529 PMID: 27250825; PubMed Central PMCID: PMC5406285.
8. McVicker BL, Bennett RG. Novel Anti-fibrotic Therapies. Front Pharmacol. 2017; 8:318. https://doi.org/10.3389/fphar.2017.00318 PMID: 28620300; PubMed Central PMCID: PMC5449464.
9. Lam M, Royce SG, Samuel CS, Bourke JE. Serelaxin as a novel therapeutic opposing fibrosis and contraction in lung diseases. Pharmacol Ther. 2018; 187:61–70. https://doi.org/10.1016/j.pharmthera.2018.02.004 PMID: 29447958.
10. Samuel CS. Relaxin: antifibrotic properties and effects in models of disease. Clin Med Res. 2005; 3(4):241–9. https://doi.org/10.3121/cmr.3.4.241 PMID: 16303890; PubMed Central PMCID: PMC1288410.
11. Pini A, Shemesh R, Samuel CS, Bathgate RA, Zauberman A, Hermesh C, et al. Prevention of bleomycin-induced pulmonary fibrosis by a novel antifibrotic peptide with relaxin-like activity. J Pharmacol Exp Ther. 2010; 335(3):589–99. https://doi.org/10.1124/jpet.110.170977 PMID: 20826567.
12. Khanna D, Clements PJ, Furst DE, Korn JH, Ellman M, Rothfield N, et al. Recombinant human relaxin in the treatment of systemic sclerosis with diffuse cutaneous involvement: a randomized, double-blind, placebo-controlled trial. Arthritis Rheum. 2009; 60(4):1102–11. https://doi.org/10.1002/art.24380 PMID: 19333948; PubMed Central PMCID: PMC3711466.
13. Chow BS, Chew EG, Zhao C, Bathgate RA, Hewitson TD, Samuel CS. Relaxin signals through a RXFP1-pERK-nNOS-NO-cGMP-dependent pathway to up-regulate matrix metalloproteinases: the additional involvement of iNOS. PLoS One. 2012; 7(8):e42714. https://doi.org/10.1371/journal.pone.0042714 PMID: 22936987; PubMed Central PMCID: PMC3425563.
14. Chen TY, Li X, Hung CH, Bahudhanapati H, Tan J, Kass DJ, et al. The relaxin family peptide receptor 1 (RXFP1): An emerging player in human health and disease. Mol Genet Genomic Med. 2020; 8(4):e1194. Epub 2020/02/27. https://doi.org/10.1002/mgg3.1194 PMID: 32100955. PubMed Central PMCID: PMC7196478.
15. Kamat AA, Feng S, Bogatcheva NV, Truong A, Bishop CE, Agoulnik AI. Genetic targeting of relaxin and insulin-like factor 3 receptors in mice. Endocrinology. 2004; 145(10):4712–20. https://doi.org/10.1210/en.2004-0515 PMID: 15256493.

16. Samuel CS, Zhao C, Bathgate RA, Du XJ, Summers RJ, Amento EP, et al. The relaxin gene-knockout mouse: a model of progressive fibrosis. Ann N Y Acad Sci. 2005; 1041:173–81. https://doi.org/10.1196/annals.1282.025 PMID: 15956703.

17. Tan J, Tedrow JR, Dutta JA, Juan-Guardela B, Nouraie M, Chu Y, et al. Expression of RXFP1 Is Decreased in Idiopathic Pulmonary Fibrosis. Implications for Relaxin-based Therapies. Am J Respir Crit Care Med. 2016; 194(11):1392–402. Epub 2016/06/17. https://doi.org/10.1164/rccm.201509-1865OC PMID: 27310652; PubMed Central PMCID: PMC5148141.

18. Giordano N, Volpi N, Franci D, Corallo C, Fioravanti A, Papakostas P, et al. Expression of RXFP1 in skin of scleroderma patients and control subjects. Scand J Rheumatol. 2012; 41(5):391–5. https://doi.org/10.3109/03009742.2012.669496 PMID: 23043266.

19. Corallo C, Pinto AM, Renieri A, Cheleschi S, Fioravanti A, Cutolo M, et al. Altered expression of RXFP1 receptor contributes to the inefficacy of relaxin-based anti-fibrotic treatments in systemic sclerosis. Clin Exp Rheumatol. 2019; 37 Suppl 119(4):69–75. PMID: 31365333.

20. Bahudhanapati H, Tan J, Dutta JA, Strock SB, Sembrat J, Alvarez D, et al. MicroRNA-144-3p targets relaxin/insulin-like family peptide receptor 1 (RXFP1) expression in lung fibroblasts from patients with idiopathic pulmonary fibrosis. J Biol Chem. 2019; 294(13):5008–22. https://doi.org/10.1074/jbc.RA118.004910 PMID: 30709904; PubMed Central PMCID: PMC6442041.

21. Karin M, Liu Z, Zandi E. AP-1 function and regulation. Curr Opin Cell Biol. 1997; 9(2):240–6. Epub 1997/04/01. https://doi.org/10.1016/s0955-0674(97)80068-3 PMID: 9069263.

22. Rajasekaran S, Vaz M, Reddy SP. Fra-1/AP-1 Transcription Factor Negatively Regulates Pulmonary Fibrosis In Vivo. PLoS One. 72012. https://doi.org/10.1371/journal.pone.0041611 PMID: 22911824

23. Westermarck J, Kahari VM. Regulation of matrix metalloproteinase expression in tumor invasion. FASEB J. 1999; 13(8):781–92. Epub 1999/05/04. PMID: 10224222.

24. Vierbuchen T, Ling E, Cowley CJ, Couch CH, Wang X, Harmin DA, et al. AP-1 Transcription Factors and the BAF Complex Mediate Signal-Dependent Enhancer Selection. Mol Cell. 2017; 68(6):1067–82. e12. Epub 2017/12/23. https://doi.org/10.1016/j.molcel.2017.11.026 PMID: 29272704; PubMed Central PMCID: PMC5744881.

25. Shao DD, Xue W, Krall EB, Bhutkar A, Piccioni F, Wang X, et al. KRAS and YAP1 converge to regulate EMT and tumor survival. Cell. 2014; 158(1):171–84. Epub 2014/06/24. https://doi.org/10.1016/j.cell.2014.06.004 PMID: 24954536; PubMed Central PMCID: PMC4110062.

26. Reese MG. Application of a time-delay neural network to promoter annotation in the Drosophila melanogaster genome. Comput Chem. 2001; 26(1):51–6. Epub 2002/01/05. https://doi.org/10.1016/s0097-8485(01)00099-7 PMID: 11765852.

27. Yu S, Yerges-Armstrong LM, Chu Y, Zmuda JM, Zhang Y. Transcriptional Regulation of Frizzled-1 in Human Osteoblasts by Sp1. PLoS One. 2016; 11(10):e0163277. https://doi.org/10.1371/journal.pone.0163277 PMID: 27695039; PubMed Central PMCID: PMC5047477.

28. Yu S, Yerges-Armstrong LM, Chu Y, Zmuda JM, Zhang Y. E2F1 effects on osteoblast differentiation and mineralization are mediated through up-regulation of frizzled-1. Bone. 2013; 56(2):234–41. https://doi.org/10.1016/j.bone.2013.06.019 PMID: 23806799; PubMed Central PMCID: PMC3758927.

29. Schneider CA, Rasband WS, Eliceiri KW. NIH Image to ImageJ: 25 years of image analysis. Nat Methods. 2012; 9(7):671–5. Epub 2012/08/30. https://doi.org/10.1038/nmeth.2089 PMID: 22930834; PubMed Central PMCID: PMC5554542.

30. Kusko RL, Brothers JF 2nd, Tedrow J, Pandit K, Huleihel L, Perdomo C, et al. Integrated Genomics Reveals Convergent Transcriptomic Networks Underlying Chronic Obstructive Pulmonary Disease and Idiopathic Pulmonary Fibrosis. Am J Respir Crit Care Med. 2016; 194(8):948–60. Epub 2016/04/23. https://doi.org/10.1164/rccm.201510-2026OC PMID: 27104832; PubMed Central PMCID: PMC5067817.

31. Zhang Y, Tedrow J, Nouraie M, Li X, Chandra D, Bon J, et al. Elevated plasma level of Pentraxin 3 is associated with emphysema and mortality in smokers. Thorax. 2021. Epub 2021/01/23. https://doi.org/10.1136/thoraxjnl-2020-215356 PMID: 33479043.

32. Messeguer X, Escudero R, Farre D, Nunez O, Martinez J, Alba MM. PROMO: detection of known transcription regulatory elements using species-tailored searches. Bioinformatics. 2002; 18(2):333–4. Epub 2002/02/16. https://doi.org/10.1093/bioinformatics/18.2.333 PMID: 11847087.

33. Sasser JM. The emerging role of relaxin as a novel therapeutic pathway in the treatment of chronic kidney disease. Am J Physiol Regul Integr Comp Physiol. 2013; 305(6):R559–65. https://doi.org/10.1152/ajpregu.00528.2012 PMID: 23883673; PubMed Central PMCID: PMC3763042.

34. Ng HH, Leo CH, Parry LJ, Ritchie RH. Relaxin as a Therapeutic Target for the Cardiovascular Complications of Diabetes. Front Pharmacol. 2018; 9:501. https://doi.org/10.3389/fphar.2018.00501 PMID: 29867503; PubMed Central PMCID: PMC5962677.

35. Ahmad N, Wang W, Nair R, Kapila S. Relaxin Induces Matrix-Metalloproteinases-9 and -13 via RXFP1: Induction of MMP-9 Involves the PI3K, ERK, Akt and PKC-ζ Pathways. Mol Cell Endocrinol. 2012; 363 (1–2):46–61. https://doi.org/10.1016/j.mce.2012.07.006 PMID: 22835547; PubMed Central PMCID: PMC3447121.

36. Bathgate RAD, Kocan M, Scott DJ, Hossain MA, Good SV, Yegorov S, et al. The relaxin receptor as a therapeutic target—perspectives from evolution and drug targeting. Pharmacology & therapeutics. 2018; 187:114–32. https://doi.org/10.1016/j.pharmthera.2018.02.008 PMID: 29458108.

37. Shaulian E, Karin M. AP-1 as a regulator of cell life and death. Nat Cell Biol. 2002; 4(5):E131–6. Epub 2002/05/04. https://doi.org/10.1038/ncb0502-e131 PMID: 11988758.

38. Eferl R, Wagner EF. AP-1: a double-edged sword in tumorigenesis. Nat Rev Cancer. 2003; 3(11):859–68. Epub 2003/12/12. https://doi.org/10.1038/nrc1209 PMID: 14668816.

39. Leppa S, Eriksson M, Saffrich R, Ansorge W, Bohmann D. Complex functions of AP-1 transcription factors in differentiation and survival of PC12 cells. Mol Cell Biol. 2001; 21(13):4369–78. Epub 2001/06/08. https://doi.org/10.1128/MCB.21.13.4369-4378.2001 PMID: 11390664; PubMed Central PMCID: PMC87096.

40. Bejjani F, Evanno E, Zibara K, Piechaczyk M, Jariel-Encontre I. The AP-1 transcriptional complex: Local switch or remote command? Biochim Biophys Acta Rev Cancer. 2019; 1872(1):11–23. Epub 2019/04/30. https://doi.org/10.1016/j.bbcan.2019.04.003 PMID: 31034924.

41. Ucero AC, Bakiri L, Roediger B, Suzuki M, Jimenez M, Mandal P, et al. Fra-2-expressing macrophages promote lung fibrosis in mice. J Clin Invest. 2019; 129(8):3293–309. Epub 2019/05/29. https://doi.org/10.1172/JCI125366 PMID: 31135379; PubMed Central PMCID: PMC6668681.

42. Eferl R, Hasselblatt P, Rath M, Popper H, Zenz R, Komnenovic V, et al. Development of pulmonary fibrosis through a pathway involving the transcription factor Fra-2/AP-1. Proc Natl Acad Sci U S A. 2008; 105(30):10525–30. Epub 2008/07/22. https://doi.org/10.1073/pnas.0801414105 PMID: 18641127; PubMed Central PMCID: PMC2492511.

43. Chiariello AM, Bianco S, Esposito A, Fiorillo L, Conte M, Irani E, et al. Physical mechanisms of chromatin spatial organization. FEBS J. 2021. Epub 2021/02/15. https://doi.org/10.1111/febs.15762 PMID: 33583147.

44. Zent J, Guo LW. Signaling Mechanisms of Myofibroblastic Activation: Outside-in and Inside-Out. Cell Physiol Biochem. 2018; 49(3):848–68. Epub 2018/09/06. https://doi.org/10.1159/000493217 PMID: 30184544; PubMed Central PMCID: PMC6611700.